


 Cite this: *RSC Adv.*, 2022, **12**, 30734

Effect of flaxseed gum on the brittleness of oleogels based on candelilla wax†

 Caihong Su, Yancai Li, Jiabin Zhu, Yuan Gao, Qi Li, Shuangkui Du and Xiuzhu Yu *

The present study aimed to decrease the brittleness of flaxseed oleogels based on candelilla wax (CLW) in combination with flaxseed gum (FG). Effects of flaxseed gum concentrations (0–0.4%) on the characteristics of flaxseed oleogels including oil binding capacity, textural, thermal, and rheological properties, and crystal polymorphisms were investigated. Higher concentrations ($\geq 0.2\%$) of FG significantly decreased the textural parameters (e.g., hardness, fracturability) of oleogels ($p < 0.05$), suggesting that FG could decrease brittleness. Rheological results indicated that all flaxseed oleogels exhibited solid-like characteristics because the elastic modulus was larger than the viscous modulus. The elastic modulus of flaxseed oleogels presented a maximum value at 0.1% gum concentration. Any increase in gum concentration beyond this concentration decreased the elastic modulus. Increasing FG concentration up to 0.4% decreased the enthalpy of flaxseed oleogels during the melting process. The β' -polymorphic form is an orthorhombic perpendicular (O_{\perp}) subcell structure. Similar β' crystal forms were observed among flaxseed oleogels, indicating that FG did not affect them negatively. The study showed that the physical properties of flaxseed oleogels based on CLW could be significantly changed by FG addition. These results provided a deeper comprehension of the novel system, which should be considered a new way to obtain healthy fats with better plasticity for food applications.

 Received 14th July 2022
 Accepted 20th October 2022

DOI: 10.1039/d2ra04341f

rsc.li/rsc-advances

1. Introduction

Oleogels are solid-like substances with a 3D network; they are formed by oleogelators through physical and chemical interactions. They have the composition of liquid oils, but can possess physicochemical properties similar to solid fats. These solid-like properties mainly attribute to diverse oleogelators. They include natural waxes,¹ monoglycerides,² phytosterols,³ proteins⁴ and polysaccharides such as ethyl-cellulose.⁵ Two main approaches are applied to achieve oleogelation, depending on the lipophilic nature of oleogelators. The direct dispersion method is only suitable for liquid-based gelators. With regard to water-soluble gelling agents such as some polysaccharides and proteins, the indirect methods (solvent exchange method or emulsion template method) may enlarge their possibility of becoming building blocks for oil structuring. Recently, oleogels have been used to produce various processed foods (including spreads, confectionery, chocolate and chocolate pastes, pastry, and meat products) because they have unique thermodynamic stability behavior, and mechanical and rheological properties.⁶ In addition, they can be used to

encapsulate and deliver bioactive nutrients such as probiotics,⁷ β -carotene,⁸ curcumin⁹ and vitamin C.¹⁰ Therefore, oleogels as promising alternatives to solid fats, which contain a large amount of unhealthy triglycerides, have been drawn increased attention.

Wax-based oleogels are formed using nature waxes as oleogelators, such as candelilla wax (CLW), rice wax, and beeswax. The well-known gelation mechanism is the immobilization of oil in the network of crystalline particles. Many studies have proven that plant waxes are the most efficient crystalline oleogelators. They can induce gelation at low critical gelling concentrations, and the obtained oleogels have good mechanical strength, physical stability and high oil-holding properties.¹¹ In addition, most waxes are low-priced, widely available and food-grade. Furthermore, they can maintain structure integrity without being altered during high-pressure homogenization process.¹² Waxes are often selected to formulate oleogels because of these advantages. In addition, wax-based oleogels applications are widely studied. They can be used to make bakery products,^{13,14} meat products,^{15,16} margarines,¹⁷ and dairy products.¹⁸ Moreover, wax-based oleogels have been regarded as a favorable delivery for the encapsulation and protection of lipophilic bioactive compounds such as curcumin and lycopene.^{9,19} Nonetheless, wax-based oleogels have some drawbacks which limit their application in foods. For example, wax-based oleogels have a high melting point when the wax concentration is greater than 3%, which is unsuitable for

Shaanxi Union Research Center of University and Enterprise for Functional Oil Engineering Technology, College of Food Science and Engineering, Northwest A&F University, 22 Xinong Road Yangling, 712100, Shaanxi, P. R. China. E-mail: xiuzhuyu@mwafu.edu.cn; Fax: +86-29-87092486; Tel: +86-29-87092308

† Electronic supplementary information (ESI) available. See DOI: <https://doi.org/10.1039/d2ra04341f>



certain foods. The residual waxy taste of the products brought by wax-based oleogels is unacceptable to consumers.²⁰ These oleogels are more prone to cause oxidation and deterioration of foods than commercial margarines, which contain large amounts of saturated fatty acids, due to the high unsaturated fatty acid content of vegetable oil. Moreover, most oleogels can match the hardness of the solid fats but lack plasticity. This finding indicates that oleogels undergo brittle fracture rather than plastic flow when a stress greater than the yield stress of the oleogels is applied.²¹ Plasticity is one of the most important characteristics of solid fats, which can provide food with good texture and mouthfeel. Therefore, future development of oleogels should be considered to decrease their brittleness and improve plasticity to satisfy the requirements of practical applications.

Flaxseed gum (FG) is a heteropolysaccharide extracted from the seeds of flaxseed plant (*Linum usitatissimum*).²² It has been widely used in the food industry in formulating nontoxic natural foods and food additives owing to its thickening, emulsification, and nutritional functional properties.²³ FG has been proven to be significantly effective in reducing blood glucose and cholesterol in patients with type 2 diabetes.²⁴ As a hydrophilic colloid, FG has “weak gel-like” property. Thus far, few studies have attempted to investigate the effect of FG on the structure properties of oleogels. Meng *et al.*²⁵ described the behavior of different thickening agents (*i.e.*, FG, xanthan gum, and Arabic gum) on the formation and properties of oleogels. These authors claimed that the mechanical strength of FG thickening emulsions was weaker than those thickened by other polysaccharides. The oleogels could be stabilized by the intramolecular or intermolecular hydrogen bonds between polysaccharides.

In the study, flaxseed oleogels with CLW as a gelator and FG as a structural modifier were developed *via* a temperature control and high-pressure homogenization technology. We aimed to obtain deep understanding of the change in FG concentrations on the structure properties of oleogels. The texture profile analysis and rheological measurements were carried out to investigate the mechanical properties (*e.g.*, hardness, fracturability, and storage modulus) of flaxseed oleogels. Differential scanning calorimetry was employed to study the thermal stability of flaxseed oleogels and X-ray diffraction was used to provide useful information on the crystal polymorphism type. The knowledge obtained would be used to develop fat mimics with desirable plasticity for nutrient-rich foods.

2. Materials and methods

2.1. Materials

FG (60% polysaccharide and 26% protein) was purchased from Henan Wanbang Industrial Co., Ltd. (Henan, China). Flaxseed oil was offered by Shaanxi Guanzhong Youfang Oil Co., Ltd. (Shaanxi, China). CLW was purchased from Shanghai Aladdin Biochemical Technology Co., Ltd. (Shanghai, China). Water was purified with a Milli-Q water purification system (Millipore Co.,

Ltd, Milford, USA). Other chemicals used were of analytical grade.

2.2. Sample preparation

The samples were prepared according to a previous study with some modifications.²⁶ The FG powder was dissolved in distilled water with stirring to provide a final concentration of 0%, 0.2%, 0.4%, 0.6%, and 0.8%. The obtained solutions were stored overnight at room temperature to assure complete hydration. Following the preparation of polysaccharide solutions, flaxseed oil and 3% CLW were held in a thermostatic bath at 80 °C for 20 min to form oil phase.

The uniform mixtures were made by adding 60% (w/w) oil phase to the prepared FG solutions, followed by mechanical stirring at 200 rpm for 10 min in electric blender (JB90-D, Guohua Instrument Experimental Factory, Jiangsu). The final FG concentrations in the systems were 0%, 0.1%, 0.2%, 0.3%, and 0.4%. Subsequently, the coarse emulsions were homogenized under high pressure (AH-BASIC, Suzhou Naluotai Instrument Co., Ltd, China), with pressures of 200 bar in the first homogenization stage and 500 bar in the second stage. These procedures were carried out at about 65 °C to prevent the solidification of mixtures in the emulsion preparation process. Then, samples were stored at 4 °C for at least 24 h prior to analysis.

2.3. Texture analysis

The newly prepared samples were poured into 10 mL beakers, gelled at room temperature and then stored at 4 °C. After refrigeration, the gels were returned to room temperature prior to texture analysis. The texture profile analysis (TPA) was carried out using a texture analyzer (TA-XT plus/50, STABLEMICVO Co. Ltd., UK) equipped with a flat stainless cylindrical probe (P/0.5R). Measurements were performed by a compression test using TPA test mode with pre-test speed of 2.0 mm s⁻¹, test speed of 1.0 mm s⁻¹, and post-test speed of 2.0 mm s⁻¹ with target depth of 10 mm. Trigger force was 3.0 g and trigger type was “auto”. Textural parameters, such as hardness, fracturability and chewiness were obtained from the texture profiles and then analyzed. For each sample, at least three replicates were formulated.

2.4. Oil binding capacity (OBC) determination

The OBC of flaxseed oleogels was measured according to Meng *et al.*²⁵ with minor modification. An approximate amount of the sample at 5.0 g was weighted in a 50 mL plastic centrifuge vial (m_1). The total mass (m_1) of the sample and the centrifuge vial was weighted. They were then centrifuged at 10 000 rpm, 25 °C for 15 min. The centrifuge vial was placed upside down on a skimmed cotton pad so that the supernatant as released liquid oil was removed completely. After removing oil, the centrifuge vial was weighted (m_2). OBC was calculated by employing eqn (1), which was according to Borriello *et al.*²⁷ with minor modification, as follows:

$$\text{OBC (\%)} = [1 - (m_1 - m_2)/(m_1 - m)] \times 100\% \quad (1)$$



where m is the mass of empty centrifuge vial, m_1 is the initial total mass of the sample and centrifuge vial, and m_2 represents the sample and centrifuge vial mass after draining the excess oil.

2.5. Thermal studies

The thermal properties of samples were studied using a Q2000 differential scanning calorimeter instrument (Waters Co., Ltd., USA). About 5.0–7.0 mg of each sample was weighed and sealed in an aluminum pan with a lid of the same material. An empty aluminum pan was set as reference. The samples were cooled from 20 °C to –50 °C at a rate of 5 °C min^{–1} under nitrogen purged at 50 mL min^{–1}. After equilibrating at –50 °C for 2 min, and the samples were heated to 25 °C at the same rate. The data including peak temperature (T_{onset}), onset temperature (T_{peak}), and total enthalpy (ΔH) of crystallization and melting were analyzed by the TA Universal Analysis software.

2.6. Rheological characteristics

Viscoelasticity of the samples was tested with a rheometer (DHR-1, Waters Instruments, USA) equipped with a temperature control system. A 40 mm diameter parallel plate was employed, setting a gap of 1000 μm . To understand the changes in the apparent viscosity, flow sweeps were performed at shear rate ranging from 0.01 s^{–1} to 100 s^{–1} for oleogels. The Herschel–Bulkley model (eqn (2))²⁸ was fitted to the flow curves, as follows:

$$\tau = \tau_0 + K\dot{\gamma}^n \quad (2)$$

where τ , τ_0 , K , γ , and n indicates the shear stress (Pa), yield stress (Pa), consistency coefficient index (Pa s ^{n}), shear rate (s^{–1}), and flow behavior index (dimensionless), respectively.

The strain sweeps were carried out at 1 Hz, setting the strain amplitude in the range of 0.01–100%. The test was performed to determine the extent of the linear viscoelastic region (LVR). To evaluate the material response, frequency sweep tests were then performed in the range of 0.01–100 rad s^{–1} at the stress value of 0.01%. The temperature sweep tests were carried out at a temperature range of 4 °C to 80 °C at a rate of 5 °C min^{–1} to measure the thermal sensitivity of samples. Each experiment was carried out two times with gels of different batches, and the elastic modulus (G') and viscous modulus (G'') were recorded.

2.7. Crystalline structure analysis

Crystalline structures of samples were obtained according to a previous study by Wang *et al.*²⁹ using a X-ray diffractometer (D8 ADVANCE A25X, Bruker, Germany). Prior to measurements, the samples were placed on the sample holders and smoothed. The X-ray diffraction (XRD) experiments were performed with a Cu source at X-ray tube ($\lambda = 1.5458 \text{ \AA}$) at 40 kV and 40 mA at environment temperature, using angular scans from 5.0° to 50.0° (2θ). Resulting data were analyzed using MDI Jade 6 software (Materials Data Inc., Livermore, USA). The crystallinity of samples was calculated according to the following eqn (3).³⁰

$$\text{Crystallinity (\%)} = \frac{\text{diffraction peak intensity}}{\text{total intensity}} \times 100 \quad (3)$$

2.8. Statistical analysis

All measurements were repeated three times. The results were expressed in mean values with standard deviations. The experimental data were analysed by the one-way analysis of variance (ANOVA) with Duncan test using IBM SPSS Statistics 20, and statistical differences were considered significant at $p < 0.05$. The curves were obtained using Origin 2018.

3. Result and discussion

3.1. Gel formation and textural properties

The flaxseed oleogels were formed when the hot mixtures containing FG solutions and oil phases were cooled down to room temperature. As shown in Fig. S1,[†] all samples were in white color with a creamy appearance. With the increase in FG concentration, the flaxseed oleogels became softer to touch but had no differences in appearance and color.

Texture measurements provided useful information on how the FG concentration influenced flaxseed oleogels' textural parameters such as hardness, fracturability and cohesiveness. The obtained results are showed in Fig. 1. The textural properties of flaxseed oleogels modified with FG decreased with increasing FG concentration overall. Hardness indicates the gel strength of the samples, and whether the gel network structure is compact. An FG concentration of 0.1% performed the largest hardness ($p < 0.05$) among oleogels without FG and other FG concentrations. Increasing the concentration of FG produced lower hardness, from $318.71 \pm 0.68 \text{ g}$ to $76.23 \pm 0.18 \text{ g}$, suggesting the formation of a weaker gel network. The probable explanation was that the higher the concentration of FG, the more obvious the aggregation of droplets in the system, and thus lower the hardness of gels.³¹ Interestingly, a reverse trend in hardness was observed with bigels based on monoglyceride-beeswax oleogel and high acyl gellan gum hydrogel, because the firmness of bigels increased with high acyl gellan gum concentration.¹⁹ Martín-Illana *et al.*³² obtained a positive relationship between the polymer concentration (pectin and hydroxypropyl methyl cellulose) and gel hardness, but this did not occur in the case of chitosan. There are only few studies which investigated the textural properties of gels as a function of hydrogelator concentration and extensive studies are needed in the future. All flaxseed oleogels exhibited fracturability during compression process. When the FG concentration was 0.1%, the fracturability was $281.95 \pm 15.20 \text{ g}$, whereas the fracturability was only $91.51 \pm 2.67 \text{ g}$ when the FG concentration reached 0.4%. Adhesiveness refers to overcoming the mutual attraction between the food surface and the materials in contact with the food. Adhesiveness decreased with increasing of FG concentration. Cohesiveness indicates that the resistance of oleogels to crumbling. Differences in cohesiveness of gels with addition of FG range from 0–0.3% were not statistically significant ($p > 0.05$). When FG concentration reached 0.4%, the



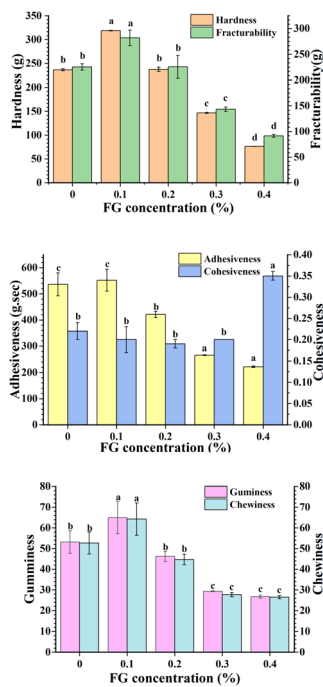


Fig. 1 Textural parameters obtained from TPA of flaxseed oleogels with different FG concentrations (0–0.4%). Different letters indicated statistically significant differences ($p < 0.05$).

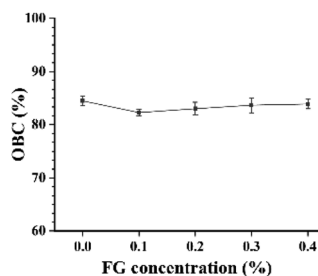


Fig. 2 OBC profile for the oleogels with different FG concentrations (0–0.4%).

cohesiveness was significantly improved. The secondary parameters (gumminess and chewiness) of the sample decreased with decreasing sample hardness. Thus, FG seemed

to change gel network derived from CLW, producing flaxseed oleogels with a softer texture.

3.2. Changes in OBC

The OBC indicated the relative capacity of oil holding of flaxseed oleogels. Studies have found the relationships between hardness and OBC, *i.e.*, the greater hardness, indicates more compact network structure of the gels. Fig. 2 shows that all samples held high OBC (>80%) regardless of FG concentration. The possible reason was that FG contained a small amount of protein and had the ability to emulsify. The increase in FG concentration promoted stronger emulsification capacity, thereby counteracting the negative effect of reduced hardness. Generally, the OBC of different flaxseed oleogels was insignificant with high oil binding levels.

3.3. Thermal stability

The samples underwent a phase transition during the temperature change, resulting in heat absorption and exothermic phenomena. Differential scanning calorimetry (DSC) was used to measure the change in heat flow during the phase transition to reflect the thermodynamic properties of the flaxseed oleogels. The T_{onset} , T_{peak} , and ΔH changes of the phase transition were analyzed and presented in Table 1.

Crystallization and melting profiles of flaxseed oleogels are shown with DSC, and the detailed data were shown in Table 1. The thermogram of flaxseed oleogels showed two narrow peaks presented below 0 °C (Fig. 3). The exotherm had a crystallization peak temperature between −38 °C and −40 °C, whereas a melting peak temperature of the endotherm was between −0.6 °C and −1.0 °C. This phenomenon, where crystallization and melting temperature of oleogels were extremely low, was ever observed in a 3% CLW dispersion in sunflower oil.³³ The peaks presented in the cooling and heating thermograms might be associated to the crystallization and melting process of the triglycerides constitutive of the flaxseed oil. The oleogels formulated with CLW (>2%) had an intense melting peak in the temperature range from 40 °C to 60 °C.^{34,35} Interestingly, no corresponding peaks in this range appeared in our preliminary experiments. The cooling cycle of the oleogels showed increasing irregular exotherms between −15 °C and −35 °C, followed by a well-defined exotherm with a peak crystallization

Table 1 Thermal parameters of flaxseed oleogels based on CLW with different FG concentrations (0–0.4%)^a

		FG concentration (%)				
DSC thermal parameters		0	0.1	0.2	0.3	0.4
Crystallization	$T_{\text{onset}}/^{\circ}\text{C}$	$-37.93 \pm 0.07^{\text{b}}$	$-37.59 \pm 0.08^{\text{a}}$	$-37.67 \pm 0.16^{\text{a}}$	$-37.59 \pm 0.01^{\text{a}}$	$-38.01 \pm 0.08^{\text{b}}$
	$T_{\text{peak}}/^{\circ}\text{C}$	$-39.55 \pm 0.03^{\text{b}}$	$-39.15 \pm 0.13^{\text{a}}$	$-39.23 \pm 0.25^{\text{a,b}}$	$-38.95 \pm 0.00^{\text{a}}$	$-39.17 \pm 0.06^{\text{a}}$
	$\Delta H/(\text{J g}^{-1})$	$83.49 \pm 8.94^{\text{a}}$	$68.93 \pm 9.41^{\text{a}}$	$45.55 \pm 1.24^{\text{b}}$	$23.66 \pm 3.95^{\text{c}}$	$23.09 \pm 2.98^{\text{c}}$
Melting	$T_{\text{onset}}/^{\circ}\text{C}$	$-1.7 \pm 0.01^{\text{a}}$	$-1.74 \pm 0.04^{\text{a}}$	$-1.67 \pm 0.11^{\text{a}}$	$-1.80 \pm 0.01^{\text{a}}$	$-1.73 \pm 0.04^{\text{a}}$
	$T_{\text{peak}}/^{\circ}\text{C}$	$-0.8 \pm 0.10^{\text{a}}$	$-0.96 \pm 1.98^{\text{a}}$	$-0.62 \pm 0.30^{\text{a}}$	$-1.02 \pm 0.05^{\text{a}}$	$-0.89 \pm 0.26^{\text{a}}$
	$\Delta H/(\text{J g}^{-1})$	$133.65 \pm 13.79^{\text{a}}$	$121.85 \pm 1.34^{\text{a,b}}$	$111.90 \pm 5.80^{\text{b}}$	$111.85 \pm 7.28^{\text{b}}$	$106.95 \pm 6.58^{\text{b}}$

^a T_{onset} : onset temperature in crystallization and melting process; T_{peak} : peak temperature in crystallization and melting process; ΔH : enthalpy of crystallization and melting. Different small letters in the same row indicate significant differences between oleogels with different concentrations of FG.



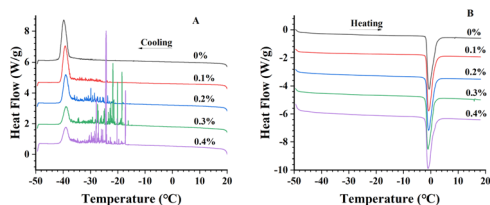


Fig. 3 DSC thermograph of flaxseed oleogels with different FG concentrations (0–0.4%) during heating at 5 °C min⁻¹. Note: the cooling (A) and the heating (B) processes.

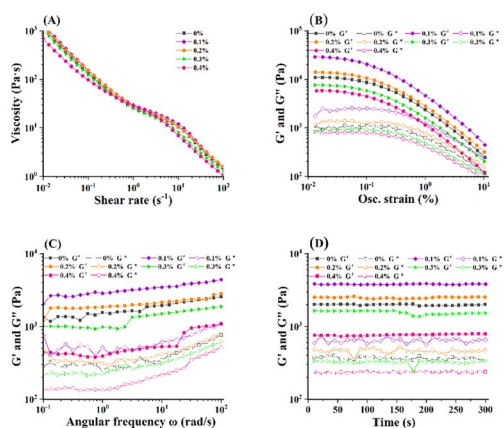


Fig. 4 Rheological properties of flaxseed oleogels with different FG concentrations (0–0.4%). Note: flow sweep (A), strain sweep (B), frequency sweep (C), and time sweep (D) curves.

temperature ≈ -39 °C. The small irregular exotherms were associated with the crystallization of polydisperse emulsified water droplets.³⁶ This finding has a significant positive correlation with the concentration of flaxseed gum because the higher concentration of FG indicates more evident phenomenon. Its presence in the oleogels indicated that the water was emulsified in larger droplets in the system with higher extent of polydispersity (*i.e.*, the irregular exotherms were more evident), particularly with 0.3% and 0.4% FG concentrations. The cooling stage of oleogels without FG did not show the presence of irregular exotherms. We considered that the high concentration of FG greatly increased the viscosity of the system, resulting in higher extent of polydispersity and even an increase in the intensity of irregular exotherms.

Table 1 shows detailed thermal parameters including T_{onset} , T_{peak} , and ΔH . In terms of T_{onset} of melting process, no significant differences ($p > 0.05$) were found among samples with FG concentrations in the range of 0.1% to 0.4%. However, within the interval of FG concentration investigated (*i.e.*, 0–0.4% FG), ΔH decreased significantly as FG concentration increased ($p < 0.05$). The ΔH of melting decreased from 133.65 ± 13.79 (J g⁻¹) to 106.95 ± 6.58 (J g⁻¹). This finding indicated that lower energy was required to destroy the sample structure. This result was in general agreement with their textural profiles.

3.4. Rheological properties

The rheological viscoelasticity of flaxseed oleogels with various FG concentrations was investigated to provide insight about their structure and utility for food applications. Fig. 4 shows the rheological properties of the flaxseed oleogels with CLW as the main oleogelator and FG as a thickening and emulsifier. Flaxseed oleogels showed shear-thinning behavior as the viscosity decreased with the increase in shear rate (Fig. 4A), suggesting that the samples exhibited non-Newtonian behavior. Similar findings were also reported by Meng *et al.*²⁵ Previous studies have proven that the viscosity of oil-in-water emulsions stabilized with FG increases with the increase in FG concentrations.^{37,38} However, with the increase in FG concentration, the viscosity of samples remained unchanged. A previous study found that no significant differences in viscosity curves of flaxseed gum solutions when process under high pressure (50–90 MPa).³⁹ The probable reason was the high shear, cavitation and turbulence forces involved during the high-pressure homogenization led to conformational transition by opening the molecule and polymer degradation.⁴⁰ Additionally, the samples prepared in this study had a relative high oil content of 60% and were solid at room temperature due to CLW. These aspects might contribute to the unusual viscous characteristics of flaxseed oleogels. However, high-pressure homogenization did not affect the crystal structure of the waxes. In this study, Herschel–Bulkley model (eqn (2)) was adopted to predict the flow behavior. The effect of FG on the model parameters is presented in Table 2. As shown in the table, the yield stress started to appear when the concentration of FG reached 0.4%. The consistency coefficient k reflects the viscosity of sample. No significant differences were found in k among the gel samples with different concentrations of FG. When the FG concentration was 0.1%, the value was maximum. This phenomenon was consistent with that in the previous study.³⁸ The flow behavior index n indicates the extent of the shear-thinning behavior. The lower the value, indicates that the extent of the shear-thinning behavior was more significant. As the FG increased from 0.1% to 0.4%, the flow index n also increased, indicating that FG addition might introduce a low extent of shear-thinning to the gels. Strain sweep could further characterize the brittleness of flaxseed oleogels. The LVRs of the different flaxseed oleogels at 1 Hz are shown in Fig. 4B, where the G' and G'' values *versus* the oscillatory strain were plotted. G' represents the solid-like behavior or elasticity of a material. All samples presented higher G' values than G'' values within the LVR, indicating that

Table 2 Herschel–Bulkley model parameters of flaxseed oleogels as affected by FG concentrations

FG concentration (%)	τ_0 (Pa)	K (Pa·s ^{n})	n	R^2
0	0	39.84	0.3051	0.9385
0.1	0	46.09	0.2938	0.9230
0.2	0	42.04	0.3071	0.9535
0.3	0	33.70	0.3025	0.9708
0.4	18.61	35.82	0.3296	0.9697



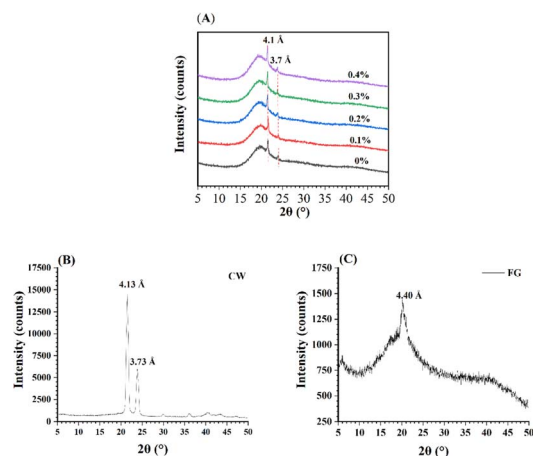


Fig. 5 XRD patterns of flaxseed oleogels based on CLW modified with different FG concentrations ((A) samples, (B) CLW, (C) FG).

Table 3 XRD for the flaxseed oleogels with different concentrations of FG (0–0.4%)

FG concentration (%)	<i>d</i> -Space (Å)		Crystallinity (%)
	Peak 1	Peak 2	
0	4.13	3.71	22.39
0.1	4.12	3.71	16.23
0.2	4.15	3.74	21.93
0.3	4.15	3.74	18.49
0.4	4.15	3.74	25.05

a typical gel network had been formed.⁴¹ The extension of LVRs determines the degree of internal structure of the samples. The plots show that all samples were weakly structured internally. The highest G' value was found for oleogel with 0.1% FG. With the increasing concentration of FG, samples showed a gradual decrease in the G' .

The plots of dynamic frequency sweep test and time sweep test of flaxseed oleogels are shown in Fig. 4C and D. For all samples, the G' and G'' values tended to increase slightly with frequencies (0.01–100 Hz), indicating that the G' and G'' of the flaxseed oleogels were frequency-dependent. The interactions among FG molecules, oil droplets, and between FG and oil droplets form a gel network structure, similar to non-covalent physical cross-linking. This phenomenon was observed in the study of Martínez-Ruvalcaba *et al.*⁴² The $\tan \delta$ values (G''/G') of all flaxseed oleogels were lower than 1.0 but higher than 0.1, suggesting a typical weak gel behavior. The G' values of oleogel containing 0.1% FG was significantly higher than that of other samples and the smallest G' was in oleogel containing 0.4% FG, in accordance with the results of the textural analysis and strain sweep results. Generally, a higher G' value indicates that the material was more resistant to deformation. Therefore, flaxseed oleogels with 0.1% and 0.2% FG presented the greatest deformation resistance among other samples. In addition, with prolonged time, the curves of G' and G'' remained parallel to the

X-axis (Fig. 4D). No cross-over points were found between G' and G'' , suggesting that the gel formation process was rapid.

3.5. Crystalline structure

XRD was used further to understand the polymorphism of flaxseed oleogels' crystals. In Fig. 5B and C, the XRD patterns of CLW and FG power were provided for comparison. A previous study showed that CLW had two distinctive sharp peaks with structure of crystalline for the orthorhombic subcell packing and *n*-hentriacontane stable polymorph.⁴³ The two diffraction peaks for CLW were at around 4.14 and 3.14 Å, which were the characteristic reflections of CLW (Fig. 5B).²⁰ The crystalline structure of CLW solids was inherited by the oleogels (Fig. 5A). However, FG powder exhibited a semi-crystalline structure with the mixture of the crystalline and amorphous area (Fig. 5C). The *d*-spacing of the crystal was calculated based on 2θ . In our study, all flaxseed oleogels showed two major peaks around 3.7 and 4.1 Å without significant differences in peak intensity. The peaks at around 3.7 and 4.1 Å indicated the presence of β' -form crystal,^{44,45} which was an orthorhombic perpendicular (O_{\perp}) subcell structure.⁴⁶ Differences in the types of crystals can affect the functional properties of fat. Among the three crystalline shapes of fat crystals, β' crystalline has better functional properties and provides lipid-rich products with good malleability, texture, and mouthfeel.⁴⁷ In addition, crystallinity changes of the flaxseed oleogels with incorporated different FG concentrations did not present a clear trend (Table 3).

4. Conclusion

The current study mainly explored the effects of flaxseed gum concentration on the brittleness of flaxseed oleogels. The flaxseed oleogels with good properties were successfully prepared by temperature control and high-pressure homogenization technology. It was found that all flaxseed oleogels were in white color with creamy appearance. The samples had significantly lower textural parameters with the increasing concentration of FG ($p < 0.05$). In particular, FG could be used to decrease the hardness and fracturability of flaxseed oleogels based on CLW, as expected. The melting temperature of the flaxseed oleogels was below 0 °C, and ΔH decreased with increasing FG concentration. This result indicated that they might be easier to shape and suitable for various food products. As the increase in the FG concentration, the rheological properties of flaxseed oleogels generally weakened. The higher FG concentration provided oleogels with stable shear-thinning behavior and weaker gel network structure. The XRD results showed that all samples had a β' crystal form and that the intensity of the diffraction peaks was unaffected by the concentration of FG. Generally, the work suggested the possibility to decrease the brittleness of flaxseed oleogels based on CLW by adding FG in oleogels. Solid fat preparations with good plasticity but less trans and saturated fats in food processing is greatly important. Nonetheless, the action mechanism and microstructure of flaxseed oleogels modified by FG were unclear. More efforts are required in the future to fully understand its functionality.



Abbreviations

CLW	Candelilla wax
FG	Flaxseed gum
TPA	Texture profile analysis
OBC	Oil binding capacity
LVR	Linear viscoelastic region
G'	Elastic modulus
G''	Viscous modulus
XRD	X-ray diffraction
DSC	Differential scanning calorimetry
T_{onset}	Onset temperature
T_{peak}	Peak temperature
ΔH	Enthalpy change
n	Flow behavior index
τ_0	Yield stress
K	Consistency coefficient index

Conflicts of interest

The authors declare that they have no known competing financial interests or personal relationships that could have appeared to influence the work reported in this paper.

Acknowledgements

The authors would like to thank the National Natural Science Foundation of China Youth Foud (No. 32201947) and Key R&D Program Projects of Shaanxi Province, China (No. 2022NY-003) for the financial support.

References

- I. Tavernier, C. D. Doan, V. D. M. Paul, B. Heyman and K. Dewettinck, *Eur. J. Lipid Sci. Technol.*, 2018, **120**, 1700393.
- A. Giacomozzi, C. Palla, M. E. Carrín and S. Martini, *Food Res. Int.*, 2020, **134**, 109231.
- L. L. Dong, M. W. Lv, X. Y. Gao, L. P. Zhang, M. Rogers, Y. Cao and Y. Q. Lan, *Food Funct.*, 2020, **11**, 9503–9513.
- K. -L. Tsung, J. Ilavsky and G. W. Padua, *J. Agric. Food Chem.*, 2020, **68**, 13276–13281.
- V. Giacintucci, C. D. D. Mattia, G. Sacchetti, F. Flamminii, A. J. Gravelle, B. Baylis, J. R. Dutcher, A. G. Marangoni and P. Pittia, *Food Hydrocolloids*, 2018, **84**, 508–514.
- A. J. Martins, A. A. Vicente, R. L. Cunha and M. A. Cerqueira, *Food Funct.*, 2018, **9**, 758–773.
- X. Q. Zhuang, N. Gaudino, S. Clark and N. C. Acevedo, *LWT–Food Sci. Technol.*, 2021, **136**, 110353.
- L. T. Li, A. Taha, M. J. Geng, Z. L. Zhang, H. C. Su, X. Y. Xu, S. Y. Pan and H. Hu, *Ultrason. Sonochem.*, 2021, **79**, 105762.
- S. Calligaris, M. Alongi, P. Lucci and M. Anese, *Food Chem.*, 2020, **314**, 126146.
- X. Wang, S. J. Wang, Y. Nan and G. Q. Liu, *Food Funct.*, 2020, **11**, 8028–8037.
- Y. Soleimanian, S. A. H. Goli, A. Shirvani, A. Elmizadeh and A. G. Marangoni, *Compr. Rev. Food Sci. Food Saf.*, 2020, **19**, 2994–3030.
- A. Schröder, J. Sprakel, K. Schroën and C. C. Berton-Carabin, *Soft Matter*, 2017, **13**, 3190–3198.
- I. Demirkesen and B. Mert, *Crit. Rev. Food Sci. Nutr.*, 2020, **60**, 2460–2479.
- J. Alvarez-Ramirez, E. J. Vernon-Carter, Y. Carrera-Tarela, A. Garcia and C. Roldan-Cruz, *LWT–Food Sci. Technol.*, 2020, **130**, 109701.
- J. Gómez-Estaca, T. Pintado, F. Jiménez-Colmenero and S. Cofrades, *LWT–Food Sci. Technol.*, 2020, **119**, 108909.
- T. L. Wolfer, N. C. Acevedo, K. J. Prusa, J. G. Sebranek and R. Tarté, *Meat Sci.*, 2018, **145**, 352–362.
- H. S. Hwang and J. K. Winkler-Moser, *J. Food Sci.*, 2020, **85**, 3293–3302.
- D. C. Z. Botega, A. G. Marangoni, A. K. Smith and H. D. Goff, *J. Food Sci.*, 2013, **78**, C1334–C1339.
- Q. M. Zhu, J. B. Gao, L. J. Han, K. X. Han, W. Wei, T. Wu, J. L. Li and M. Zhang, *Food Chem.*, 2021, **365**, 130419.
- J. D. Pérez-Martínez, M. Sánchez-Becerril, A. G. Marangoni, J. F. Toro-Vazquez, J. J. Ornelas-Paz and V. Ibarra-Junquera, *Food Res. Int.*, 2019, **122**, 471–478.
- A. R. Patel, R. A. Nicholson and A. G. Marangoni, *Curr. Opin. Food Sci.*, 2020, **33**, 61–68.
- J. Liu, Y. Y. Shim, T. J. Tse, Y. Wang and M. J. T. Reaney, *Trends Food Sci. Technol.*, 2018, **75**, 146–157.
- F. Rashid, Z. Ahmed, S. Hussain, J. Y. Huang and A. Ahmad, *Carbohydr. Polym.*, 2019, **215**, 29–38.
- G. Thakur, A. Mitra, K. Pal and D. Rousseau, *Int. J. Food Sci. Nutr.*, 2009, **60**, 126–136.
- Z. Meng, K. Y. Qi, Y. Guo, Y. Wang and Y. F. Liu, *Food Chem.*, 2018, **246**, 137–149.
- C. H. Liu, Z. J. Zheng, Y. F. Shi, Y. Zhang and Y. F. Liu, *Food Chem.*, 2021, **345**, 128811.
- A. Borriello, P. Masi and S. Cavella, *LWT–Food Sci. Technol.*, 2021, **152**, 112165.
- R. Farahmandfar, M. Asnaashari, A. Taheri and T. K. Rad, *Int. J. Biol. Macromol.*, 2019, **121**, 609–615.
- L. Q. Wang, Y. X. Wen, C. H. Su, Y. Gao, Q. Li, S. K. Du and X. Z. Yu, *RSC Adv.*, 2022, **12**, 8987–8995.
- Y. Lu, L. K. Mao, Z. Q. Hou, S. Miao and Y. X. Gao, *Food Eng. Rev.*, 2019, **11**, 245–258.
- L. J. Han, H. Chen, S. Liu, Y. T. Qi, W. N. Zhang, J. B. He, Q. Wang and C. Qi, *J. Food Sci.*, 2018, **39**, 14–19.
- A. Martín-Illana, F. Notario-Pérez, R. Cazorla-Luna, R. Ruiz-Caro and M. D. Veiga, *Pharmaceutics*, 2019, **11**, 232.
- J. F. Toro-Vazquez, J. A. Morales-Rueda, E. Dibildox-Alvarado, M. Charó-Alonso, M. Alonzo-Macias and M. M. González-Chávez, *J. Am. Oil Chem. Soc.*, 2007, **84**, 989–1000.
- T. L. T. da Silva, D. B. Arellano and S. Martini, *Food Biophys.*, 2019, **14**, 30–40.
- A. K. Rodríguez-Hernández, J. D. Pérez-Martínez, J. A. Gallegos-Infante, J. F. Toro-Vazquez and J. J. Ornelas-Paz, *Carbohydr. Polym.*, 2021, **252**, 117171.



Paper

- 36 M. L. García-Ortega, J. F. Toro-Vazquez and S. Ghosh, *Food Res. Int.*, 2021, **150**, 110763.
- 37 M. Wang, M. Q. Feng, K. Jia, J. Sun, X. L. Xu and G. H. Zhou, *Food Hydrocolloids*, 2017, **67**, 54–62.
- 38 Y. Wang, D. Li, L. J. Wang and B. Adhikari, *J. Food Eng.*, 2011, **104**, 56–62.
- 39 Y. Wang, D. Li, L. J. Wang and J. Xue, *Carbohydr. Polym.*, 2011, **83**, 489–494.
- 40 N. Lagoueyte and P. Paquin, *Food Hydrocolloids*, 1998, **12**, 365–371.
- 41 A. J. Martins, M. A. Cerqueira, R. L. Cunha and A. A. Vicente, *Food Funct.*, 2017, **8**, 4241–4250.
- 42 A. Martínez-Ruvalcaba, E. Chornet and D. Rodrigue, *Carbohydr. Polym.*, 2007, **67**, 586–595.
- 43 L. L. Serrato-Palacios, J. F. Toro-Vazquez, E. Dibildox-Alvarado, A. Aragón-Piña, M. D. R. Morales-Armenta, V. Ibarra-Junquera and J. D. Pérez-Martínez, *J. Am. Oil Chem. Soc.*, 2015, **92**, 533–540.
- 44 L. S. K. Dassanayake, D. R. Kodali, S. Ueno and K. Sato, *J. Am. Oil Chem. Soc.*, 2009, **86**, 1163–1173.
- 45 M. X. Zhao, Y. Lan, L. Q. Cui, E. Monono, J. J. Rao and B. C. Chen, *Food Chem.*, 2020, **309**, 125704.
- 46 C. H. Liu, Z. J. Zheng, F. Zaaboul, C. Cao, X. L. Huang and Y. F. Liu, *Food Funct.*, 2019, **10**, 5413–5425.
- 47 M. Ögütcü, N. Arifoğlu and E. Yılmaz, *J. Am. Oil Chem. Soc.*, 2015, **92**, 459–471.

